The nucleocytoplasmic shuttling protein CIZ reduces adult bone mass by inhibiting bone morphogenetic protein–induced bone formation

Mikihiko Morinobu,[1] Tetsuya Nakamoto,[4] Kazunori Hino,[1] Kunikazu Tsuji,[1] Zhong-Jian Shen,[1] Kazuhisa Nakashima,[1] Akira Nifuji,[1] Haruyasu Yamamoto,[5] Hisamaru Hirai,[4] and Masaki Noda[1,2,3]

[1]Department of Molecular Pharmacology, Tokyo Medical and Dental University, [2]Center of Excellence Program for Frontier Research on Molecular Destruction and Reconstruction of Tooth and Bone, [3]Integrated Action Initiative, Core to Core Program for Advanced Bone and Joint Science, Japan Society for Promotion of Science, Tokyo 101-0062, Japan
[4]University of Tokyo, Tokyo 113-8655, Japan
[5]Ehime University, Ehime 791-0295, Japan

Osteoporosis is a major health problem; however, the mechanisms regulating adult bone mass are poorly understood. Cas-interacting zinc finger protein (CIZ) is a nucleocytoplasmic shuttling protein that localizes at cell adhesion plaques that form where osteoblasts attach to substrate. To investigate the potential role of CIZ in regulating adult bone mass, we examined the bones in CIZ-deficient mice. Bone volume was increased and the rates of bone formation were increased in CIZ-deficient mice, whereas bone resorption was not altered. CIZ deficiency enhanced the levels of mRNA expression of genes encoding proteins related to osteoblastic phenotypes, such as alkaline phosphatase (ALP) as well as osterix mRNA expression in whole long bones. Bone marrow cells obtained from the femora of CIZ-deficient mice revealed higher ALP activity in culture and formed more mineralized nodules than wild-type cells. CIZ deficiency enhanced bone morphogenetic protein (BMP)–induced osteoblastic differentiation in bone marrow cells in cultures, indicating that BMP is the target of CIZ action. CIZ deficiency increased newly formed bone mass after femoral bone marrow ablation in vivo. Finally, BMP-2–induced bone formation on adult mouse calvariae in vivo was enhanced by CIZ deficiency. These results establish that CIZ suppresses the levels of adult bone mass through inhibition of BMP-induced activation of osteoblasts.

CORRESPONDENCE
Masaki Noda:
noda.mph@mri.tmd.ac.jp

Abbreviations used: ALP, alkaline phosphatase; BMP, bone morphogenetic protein; CIZ, Cas-interacting zinc finger protein; COL, type I collagen; LRP5, low-density lipoprotein receptor-related protein 5; OPN, osteopontin; rh, recombinant human; TRAP, tartrate-resistant acid phosphatase.

Osteoporosis is one of the major health problems in our modern society with respect to the large number of patients as well as a huge medical cost (1–3). Bone loss in bed-ridden patients with age-related problems such as cerebrovascular diseases or osteopenia due to estrogen depletion after menopause increase the risk of fractures (4–6). More importantly, low levels of adult (peak) bone mass also increase the risk of fractures. However, limitation in the knowledge on the molecules acting as signaling factors to determine adult bone mass has hampered the progress in understanding the mechanisms that control adult bone mass levels.

Osteoblasts attach to bone and regulate extracellular environment, while they are also controlled by bone via membrane-bound attachment proteins, which form adhesion plaques in these cells. These molecules are one of the candidates to regulate osteoblasts by conveying attachment signals from bone (7, 8). Thus, bone matrix could give signals from outside the body to the cells (9, 10) either through matrix-residing cytokines, through these attachment machineries, or both. Such extracellular matrix-derived signals regulate osteoblastic cell mostly, if not exclusively, via transcriptional events (11–14). Therefore, molecules that could localize at adhesion plaques and, at the same time, modulate transcription in nuclei are intriguing candidates that participate in the regulation of osteoblastic function and bone mass.

The Journal of Experimental Medicine

Cas-interacting zinc finger protein (CIZ) is a nucleocytoplasmic shuttling protein and it was initially identified by far-western screening of a rat 3Y1 cDNA library using SH3 domain of $p130^{cas}$ as a probe (15). As expected based on its interaction with $p130^{cas}$, CIZ colocalizes with vinculin and other adhesion-related proteins at adhesion plaques (15). Interestingly, CIZ contains nuclear localization signal as well as five to eight zinc fingers (15–17), binds to a consensus sequence, (G/C)AAAAA, and activates transcription via promoters of the genes encoding matrix metalloproteinases such as MMP-7 (15).

CIZ is expressed in osteoblasts in culture. However, its function has not yet been clear as CIZ overexpression in vitro has been either reported to activate or to inhibit osteoblastic activities depending on experimental conditions (16, 18, 19). Thus, in vivo physiological function of CIZ in bone has not yet been determined. To obtain insights into the role of CIZ in bone in vivo, we investigated the bone in the CIZ-deficient mice.

RESULTS

X-ray examinations of the bone revealed that gross morphology of the femora in CIZ-KO mice was similar to that in wild type (Fig. 1, A and B). Body weight in CIZ-KO mice was ∼10% less at the 8-wk time point, whereas it caught up with the weight of wild-type mice by 50 wk (Fig. 1 C). X ray of the long bone revealed that trabecular spicules present in the distal end of femora were observed to be denser in CIZ-KO compared with wild type (Fig. 2 A). Similarly, femoral neck (Fig. 2 A) was more radiopaque in CIZ-KO compared with wild type. Radiopacity levels in the distal ends of the femur (condyle regions) were similar between the two genotypes (Fig. 2 A).

To further visualize the changes in the trabecular bone structures in the femora, two-dimensional microCT examination was conducted in the metaphyseal regions of the femora within a midsagittal plane. This demonstrated that more cancellous bone was present in the femora in CIZ-KO mice than wild-type mice (Fig. 2 B). Quantification of the trabecular bone on the microCT sections of the femora (Fig. 2 B, rectangle) indicated that BV/TV levels were increased by ∼40% in CIZ-KO mice (Fig. 2 C). Increase was not limited to long bones as microCT examination of the lumbar vertebrae indicated ∼15% increase in trabecular bone mass (Fig. 2, D and E).

To examine whether CIZ deficiency–induced increase in bone volume could be due to reduction in bone resorption, histomorphometric analysis was conducted to obtain bone resorption parameters. Osteoclast morphology (not depicted) as well as quantitative bone resorption parameters, including osteoclast number per bone surface (N.Oc/BS) and osteoclast surface per bone surface (Oc.S/BS) in the histological sections, were similar between wild-type and CIZ-deficient mice (Fig. 3, A and B). Thus, bone resorption would not be a major target of CIZ action. In contrast with

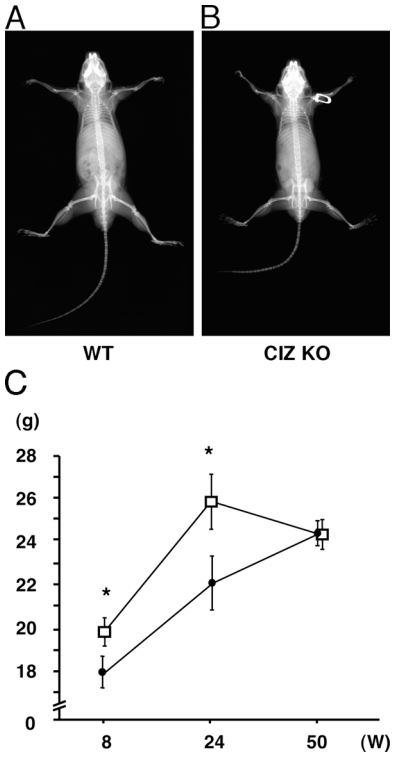

Figure 1. Radiological examination of CIZ KO mice. (A) Soft X-ray image of WT mice. (B) Soft X-ray image of CIZ KO mice. (C) Time course of the body weight in CIZ-KO mice and wild-type mice.

the bone resorption parameters, histomorphometry on bone formation parameters in CIZ-deficient mice based on calcein double labeling indicated that the bone formation rate and mineral apposition rate were enhanced in CIZ-KO mice in comparison with those in wild-type mice (Fig. 4, A–C). Therefore, CIZ deficiency enhances specifically bone formation activity in vivo without altering bone resorption to increase trabecular bone volume.

We further investigated whether CIZ deficiency enhances osteoblastic activity in a cell-autonomous manner. For this purpose, bone marrow cells were obtained from the femora of wild-type and CIZ-deficient mice and were cultured in the presence of ascorbic acid and β-glycerophosphate. Alkaline phosphatase (ALP) activity was measured after 10 d in cultures. Bone marrow cells from CIZ-KO mice revealed higher basal levels ALP activity than the cells from wild-type mice (Fig. 5).

To examine whether such CIZ deficiency–induced enhancement of ALP activity could be translated into alteration in calcified tissue formation, nodule formation assays were conducted. As shown in Fig. 6 A, CIZ deficiency enhanced the formation of alizarin red–S-positive mineralized nodules in the bone marrow cells in culture. Quantification of the alizarin red-positive nodules revealed approximately threefold enhancement of the nodule formation in CIZ-deficient

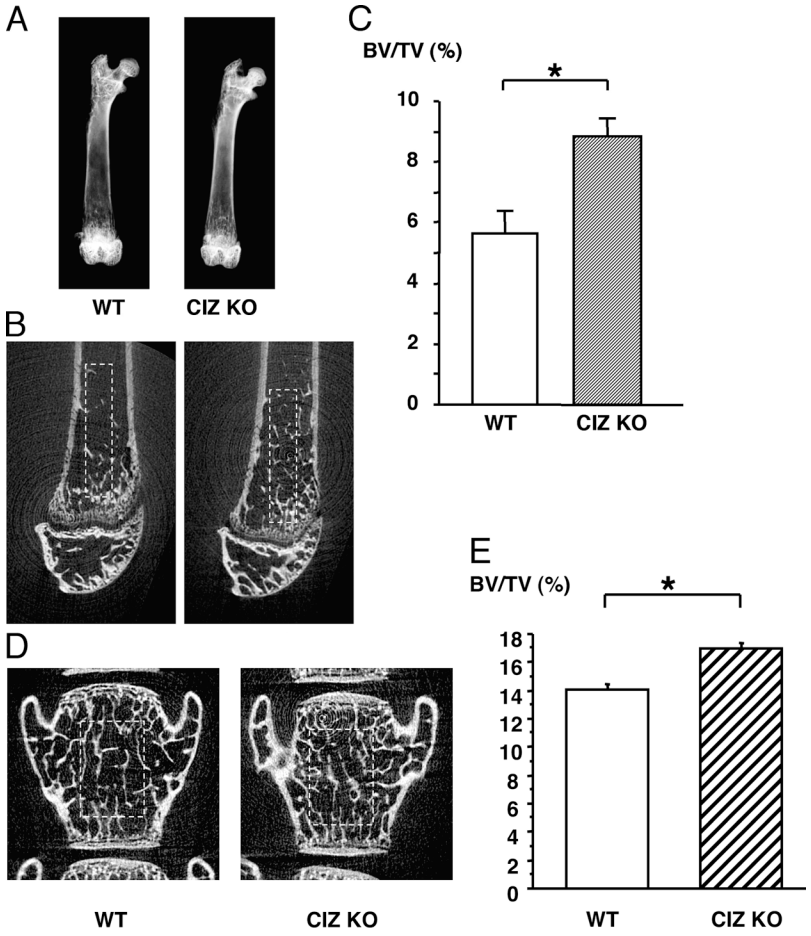

Figure 2. Trabecular bone volume of the femora is increased in CIZ KO mice. (A) Soft X-ray image of the femora of WT and CIZ-KO mice. The two bones shown in A were subjected to X-ray exam on the same X-ray film and, therefore, X-ray exposure (power [i.e., volts/amperes], exposure time), developing solution, developing time, and temperature were exactly the same. Trabecular bone spicule, femoral neck, and condyle region are depicted. Two-dimensional microCT images of the midsagittal planes of the distal regions of the femora (B) or vertebrae (D) of WT and CIZ-KO mice. Fractional trabecular BV/TV was quantified based on the image analysis of two-dimensional microCT images of the femora (C) or vertebrae (E) of WT and CIZ-KO mice. Analyses were conducted in the rectangular area shown in B and D. Asterisk indicates statistically significant difference ($P < 0.05$).

bone marrow cells (Fig. 6 B). These data indicate that CIZ deficiency enhances osteoblastic activity in a cell-autonomous manner. We also performed bone marrow cultures to examine the effect of CIZ deficiency on osteoclastogenesis. CIZ deficiency did not alter the levels of tartrate-resistant acid phosphatase (TRAP)-positive multinucleated cell formation in culture, indicating that CIZ deficiency does not target cells in osteoclast lineage (Fig. 6 C).

To explore the molecular bases for CIZ deficiency–induced enhancement in bone formation in vivo, we examined expression profile of osteoblastic phenotype-related genes in the bone of these mice. Total RNA was extracted from whole humeri and was subjected to RT-PCR analysis. The mRNA expression levels of osteoblastic phenotype-related genes such as type I collagen (COL), ALP, and osteopontin (OPN), as well as upstream transcription factor gene, osterix (OSX), were enhanced in CIZ-KO mice (Fig. 7, A and B). These data reveal that the increase in bone-forming activity in the cells in CIZ-deficient mice in vivo at least in part is based on the enhancement of expression of the genes encoding osteoblastic phenotype-related proteins as well as upstream osteoblastic transcription factor.

To examine the mechanism of how CIZ deficiency affects osteoblastic activities, effects of CIZ deficiency on bone morphogenetic protein (BMP) actions were examined in vitro and in vivo. First, CIZ deficiency effects on BMP actions were examined in the bone marrow cells in culture. ALP activity in wild-type bone marrow cells was enhanced by approximately threefold by BMP treatment (100 ng/ml recombinant human [rh]BMP-2 for 10 d; Fig. 8). Such BMP-enhanced ALP activity levels in wild-type cells were comparable to ALP activity levels in vehicle-treated CIZ-deficient cells, indicating that the absence of CIZ per se resulted in the enhancement of ALP levels as potently as BMP

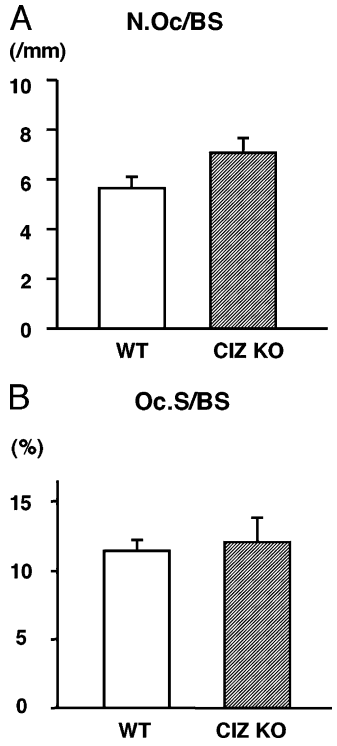

Figure 3. Quantification of the osteoclastic parameters in the trabecular bone of the femora of WT and CIZ-KO mice. Sections of the femora of WT and CIZ-KO mice were subjected to TRAP and Fast green staining followed by histomorphometry. (A) Quantification of N.Oc/BS in the bone marrow cavity of WT and CIZ-KO mice. (B) Quantification of Oc.S/BS in the bone marrow cavity of WT and CIZ-KO mice.

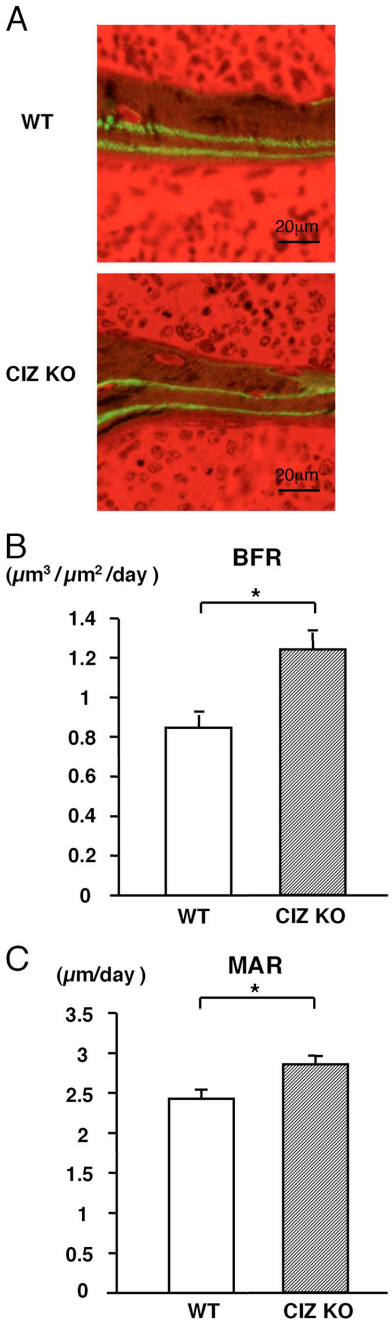

Figure 4. Bone formation rate and mineral apposition rate are increased in CIZ KO mice. (A) Cross sections of the femora of WT and CIZ-KO mice. Calcein labeling was conducted and labeled lines were visualized and measurement was performed under fluorescent microscopy. (B) Quantification of bone formation rate (BFR) in the secondary spongiosa of WT and CIZ-KO mice. (C) Quantification of mineral apposition rate (MAR) in the secondary spongiosa of WT and CIZ-KO mice. Asterisks indicate statistically significant difference ($P < 0.05$).

treatment. BMP treatment of CIZ-deficient cells further enhanced ALP levels up to threefold compared with those in BMP-treated wild-type cells (up to ninefold compared with vehicle-treated wild-type cells). Thus, for the same BMP treatment, presence versus absence of CIZ resulted in one- versus threefold increase in ALP activity levels, respectively, indicating that CIZ deficiency enhances BMP effects in vitro in a cell-autonomous manner.

Furthermore, we asked whether such in vitro CIZ deficiency effects on BMP actions can be translated into bone formation in vivo. For this purpose, bone marrow ablation was conducted because BMP expression was reported to be observed during bone regeneration in bone marrow ablation experiments (20). Bone marrow ablation was performed on the femora of wild-type and CIZ-KO mice, and the bones were examined using two-dimensional microCT 10 d later. Images of CIZ-deficient mice revealed denser newly formed trabecular bone patterns in the ablated area in the femora after bone marrow ablation compared with wild type (Fig. 9 A, rectangular area). Quantification of the newly formed trabecular bone (BV/TV) indicated that fractional bone volume in wild-type mice was increased by 3.0-fold relative to intact contralateral femora after ablation, whereas CIZ deficiency enhanced the increase in fractional bone volume by 3.7-fold relative to intact contralateral femora (Fig. 9 B, $P < 0.05$), even though the basal intact bone mass levels

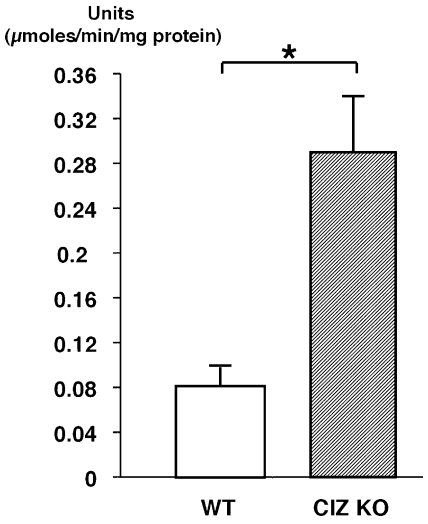

Figure 5. CIZ deficiency enhances basal ALP activity levels in bone marrow cells. Bone marrow cells were cultured as described in Materials and methods for 10 d. The media were changed every 3 d. ALP activities were measured in cells cultured in six wells and the values were normalized against protein concentrations. Asterisk indicates statistically significant difference ($P < 0.05$).

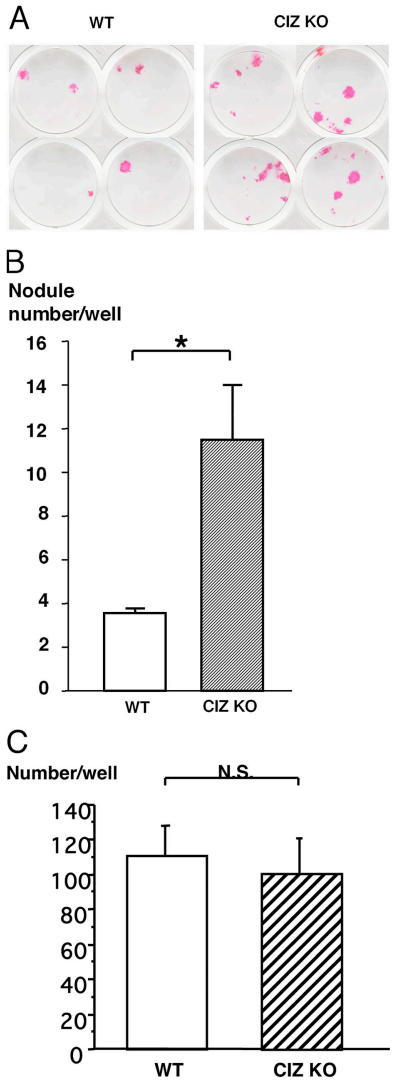

Figure 6. Formation of mineralized nodules in culture is enhanced by CIZ deficiency. (A) Bone marrow cells were cultured in the mineralization medium for 2 wk and at the end of the culture, mineralized nodules were visualized by Alizarin red-S staining. The data represent one out of three independent experiments with similar results using cells from different mice. (B) Quantification of the number of the mineralized nodules in cultures. Asterisk indicates statistically significant difference ($P < 0.05$). (C) Quantification of the number of the TRAP-positive multinucleated cells developed in culture. Osteoclastogenesis was conducted using bone marrow cells obtained from wild-type and CIZ KO mice.

were higher than wild type. These observations indicate that CIZ deficiency enhances new trabecular bone formation in the ablation-induced bone regeneration model in vivo.

As the bone marrow ablation model does not specifically address whether CIZ deficiency–induced in vivo bone formation is through modulation of BMP actions alone or through bone formation in response to a mixture of injury-related cytokines, we tested whether CIZ deficiency enhances BMP-induced bone formation directly in vivo. 5 μg rhBMP-2 was injected onto the calvariae of wild-type and CIZ-KO mice to induce orthotopic bone formation. The rhBMP-2 injection–induced de novo bone formation was evaluated based on soft X-ray images using an image analyzer and was expressed as the area of the newly formed bone. Direct rhBMP-2 injection produced new bone, which was detected on soft X-ray images as shown in Fig. 10 A (arrow). Quantification of the area of the newly formed bone indicated that approximately twofold greater bone was formed by rhBMP-2 injection onto the calvariae of CIZ-deficient mice than that produced by rhBMP-2 injection onto the wild-type calvariae (Fig. 10 B). These data demonstrate that BMP-2–induced bone formation is enhanced in the absence of CIZ, indicating that CIZ suppresses BMP-signaling in vivo.

DISCUSSION

Our data revealed that deficiency in CIZ increased basal bone mass in adult mice. This phenotype was through the enhancement of bone formation in vivo, increased mineralized nodule formation in bone marrow cells, and elevated expression levels of the genes encoding osteoblastic phenotype-related marker proteins including COL1, ALP, OPN, and OSX in bone in vivo. CIZ deficiency also enhanced bone marrow ablation-induced new bone formation in vivo as well as BMP injection–induced de novo osteogenesis in adult mice. Thus, CIZ acts as an inhibitor of bone formation in adult mice in vivo at least in part through its suppression of BMP actions.

CIZ localizes at adhesion plaques, transfers into nuclear compartments, binds to consensus DNA sequences, and activates promoters of the genes encoding enzymes that degrade

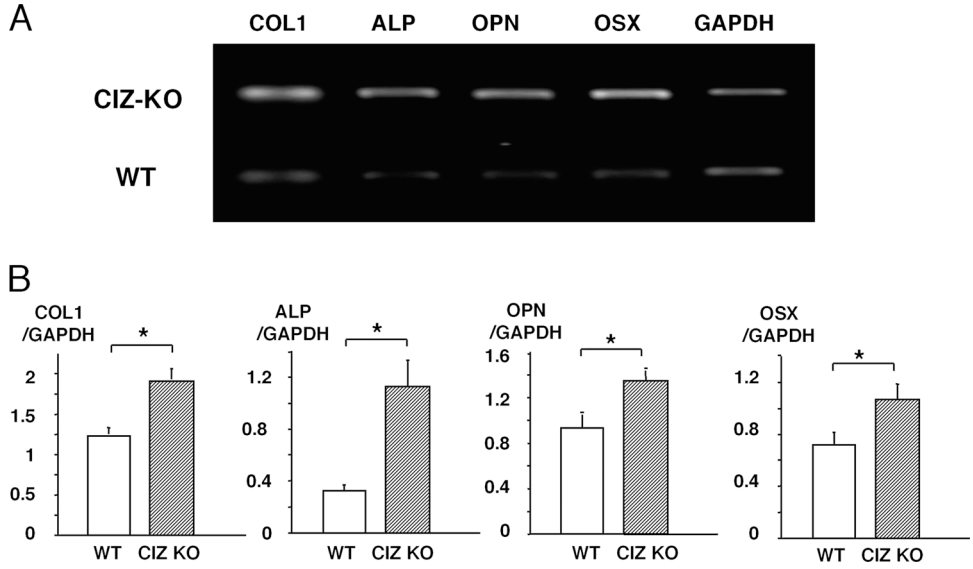

Figure 7. RT-PCR analysis of the gene expression in the bone in WT and CIZ-deficient mice. (A) Total RNA was extracted from humeri, and RT-PCR was performed using primer sets for murine OPN, ALP, COL1, OSX, or GAPDH genes. The amplified RT-PCR products were 244 bp of murine COL1, 460 bp of ALP, 460 bp of OPN, 473 bp of OSX, or 452 bp of GAPDH. The samples were electrophoresed in a 1% agarose gel plate and stained with ethidium bromide to visualized the bards. (B) Quantification of the expression on the genes shown in A. Asterisks indicate statistically significant difference ($P < 0.05$).

matrix proteins (15). As CIZ is expressed in cultured osteoblasts (17–19), this protein was thought to be a modulator of osteoblastic function. However, there was an ambiguity regarding CIZ actions in vitro because CIZ was reported to regulate expression of osteoblast-related genes positively or negatively depending on culture conditions (18, 19). Thus, in vitro overexpression experiments failed to determine CIZ function in osteoblasts. Our data in this paper conclusively indicated that CIZ deficiency enhanced adult bone volume levels in vivo. Therefore, CIZ is an inhibitory determinant for adult bone mass in vivo. CIZ deficiency enhances basal as well as BMP-induced alkaline phosphates activities in osteoblasts in culture. This implies that in vivo observations on the elevation of basal bone mass in CIZ-deficient mice as well as CIZ deficiency enhancement in BMP-induced bone formation on calvaria in vivo would be reflecting cell-autonomous actions of CIZ. Furthermore, we have observed previously in cultured osteoblasts that CIZ overexpression suppressed Smad-dependent activation of transcription (19). In the present work, CIZ deficiency enhanced bone formation and mineral apposition rates without altering osteoclast number and osteoclast surface in vivo. Therefore, CIZ suppresses adult bone mass levels by reduction in osteoblastic activity through the inhibition of BMP actions via interference of Smad activities.

Several signaling mechanisms have been reported to regulate adult bone mass in the last several years. Low-density lipoprotein receptor-related protein 5 (LRP5) acts as a coreceptor for Wingless-Int family member signaling, and loss of function mutation in LRP5 gene leads to osteoporosis. Similarly, other types of LRP5 mutation blocks the binding of dickkopf (DKK), an inhibitor of LRP5, and leads to increase in bone mass in humans. Another group of molecules is involved in negative regulation of adult bone mass via suppression of function; these include inhibitors of BMP such as Tob (21, 22). It is intriguing that multiple molecules such as Tob and CIZ are involved in suppression of osteoblastic functions.

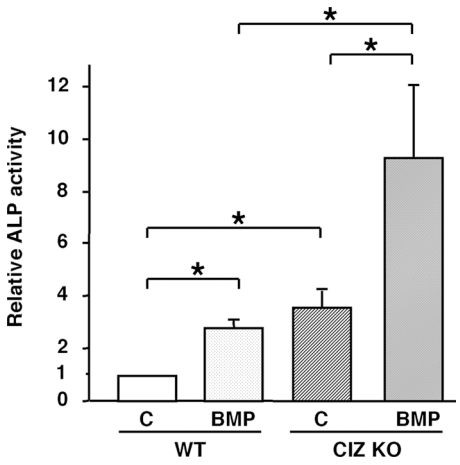

Figure 8. CIZ deficiency enhances BMP-2–induced ALP expression in bone marrow cells. Bone marrow cells were cultured in the absence or presence of 100 ng/ml BMP-2 for 10 d. The media were changed every 3 d. ALP activities were measured in the bone marrow cells and the values were normalized against protein concentrations. Data are expressed as fold induction of the ALP activities relative to WT control samples. Asterisks indicate statistically significant difference ($P < 0.05$).

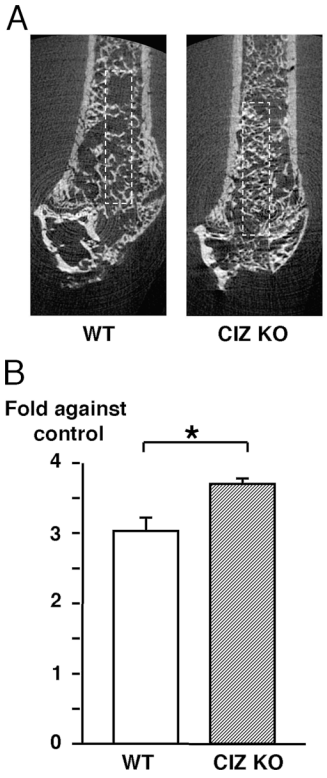

Figure 9. New bone formation in vivo after marrow ablation is enhanced in CIZ-deficient mice. (A) Two-dimensional microCT images of the midsagittal planes of the distal regions of the femora after 10 d after ablation surgery in WT and CIZ-KO mice. (B) Fractional trabecular BV/TV was quantified based on the image analysis of two-dimensional microCT images of the intact and ablated femora after 10 d after ablation surgery in WT and CIZ-KO mice. Analyses were conducted in the rectangular area shown in A. Data are expressed as fold in BV/TV of ablated side bone relative to their control (nonablated side) bone. Asterisk indicates statistically significant difference ($P < 0.05$).

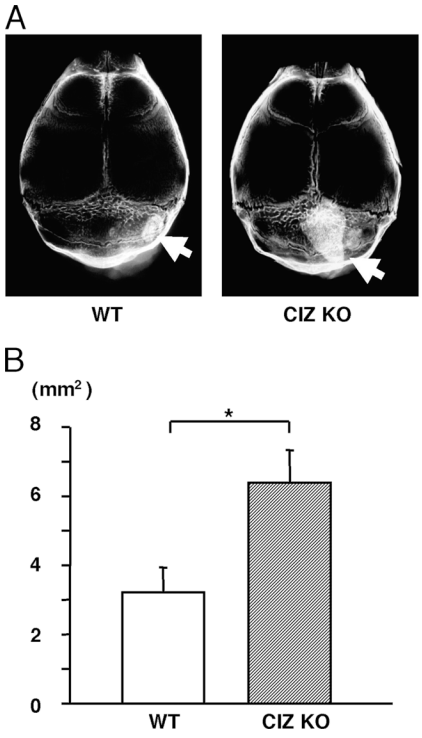

Figure 10. CIZ deficiency enhances BMP-2–induced bone formation in vivo. (A) Soft X-ray image of the calvariae of WT and CIZ-KO mice after 10 d of rhBMP-2 injection. Arrows indicate newly formed bone. (B) Quantification of the amount of newly formed bone as an area based on the soft X-ray image of calvariae of WT and CIZ-KO mice. Asterisk indicates statistically significant difference ($P < 0.05$).

Bone is the storage site for BMP and, thus, the cells in bone could be subjected to continuous and possibly excessive exposure to BMP-driven stimuli. CIZ and Tob may partly block such excessive BMP signals and, thus, prevent abnormal or ectopic bone formation. Such negative regulation of BMP action by at least two distinct effectors, in this case CIZ and Tob, could be an important biological back-up pathway. This makes us speculate about the presence of strong potency in BMP action during the determination in adult bone mass. As deletion of even one of the two molecules CIZ and Tob results in exhibition of bone phenotype, simultaneous presence of both of the two is necessary for normal bone mass maintenance. Furthermore, we observed that both CIZ and Tob expression levels in osteoblasts in cultures are enhanced by BMP treatment. Thus, these two molecules form negative feedback circuits with BMP separately or in parallel. It can be observed in other biological systems that growth factors stimulate biological functions of cells while these molecules simultaneously enhance expression of inhibitors for their own activities (23–26). The balanced activities of both accelerators (stimulating cytokines) and decelerators (their inhibitors) would determine the normal balance in the biological functions of organs (in this case, bone). To our knowledge, CIZ is the first attachment- and transcription-related molecule that inhibits osteoblastic function in adult bone in vivo.

BMP is an important molecule in the body in various aspects. BMP is required for the maintenance of bone to support the body or to protect internal organs. BMP also regulates morphogenesis during embryonic development. In accordance with such a variety of BMP actions, numerous groups of BMP inhibitors have been identified. One group includes soluble BMP inhibitors such as noggin, chordin, SOST, and gremlin, which act outside the cells. These molecules inhibit BMP signaling via binding to BMP ligands to prevent their binding to their cognate receptors (27–29). BMP3 binds to BMP receptor and inhibits bone formation. Other groups consist of inhibitory Smad proteins, such as Smad6 and Smad7. These negative Smads inhibit intracellular BMP signaling by binding to BMP receptors or regulatory Smads (30, 31). A recently identified group contains proteins such as Tob, which acts as a Smad repressor to inhibit BMP signaling at the level of the nuclear transport or

transcription (31). CIZ is special and distinct from other proteins because it localizes at adhesion plaques and simultaneously activates gene expression in addition to Smad modulation (19). It is also unique in terms of its localization at nuclear matrix (15). Thus, CIZ should be considered as a unique class of BMP inhibitor in vivo.

It is notable that CIZ deficiency did not result in major alterations in skeletal morphogenesis during embryonic stages. In the case of other BMP inhibitors, such as noggin, its deficiency causes hypertrophy of cartilage and severe fusion of joints. These knockout mice do not survive after birth (31). This may imply that CIZ deficiency could be backed up by the presence of other BMP inhibitors during the early period of life when embryonic development of the skeleton is taking place. Alternatively, CIZ-deficient mice may not have an obvious (major) skeletal phenotype in embryonic stage because of the rapid growth during that period of life. Our observations revealed that CIZ action is more important in bone metabolism in "adulthood" than in the embryonic stage, even when the target is BMP. In fact, we observed that high bone mass phenotype could be detectable even in mice of >50 wk old (unpublished data). These facts suggest that different BMP inhibitors would have diverse roles depending on time and location as well as cellular backgrounds. As most age-related diseases, including osteoporosis, affect individuals who grow and live normally up to adult stage, the roles of molecules, such as CIZ, could be critical for considering the pathogenesis of age-related bone diseases in human adults. CIZ-deficient mice also revealed defects in spermatogenesis (32). However, except for that, bone is the only organ to reveal a phenotype in these mice. Even for males, spermatogenesis may not be a major problem in an aged population; therefore, it would be of interest to contemplate development of new drugs to target against CIZ for osteoporosis in aged patients.

In conclusion, our observations demonstrate that CIZ deficiency enhances the levels of adult bone mass and bone formation. This was observed to be due to enhancement in the BMP signaling pathway in vivo and in osteoblasts in a cell-autonomous manner. Thus, CIZ would act as a critical suppressor for BMP signaling in osteoblastic function in adult in vivo.

MATERIALS AND METHODS

Animals. CIZ-deficient mice were produced by Nakamoto et al. (32). Wild-type and CIZ-deficient mice in a DBA × C57BL/6 F2 background were derived from the original heterozygous cross. These mice were maintained as separate colonies. The mice were kept under controlled housing condition at 24°C on 12:12 light/dark cycles with the light cycle starting at 7:00 a.m., fed with standard laboratory chow (MF; Oriental Yeast), and given tap water. CIZ-deficient and wild-type female mice (8 wk old) were used in most of the experiments. For body weight data and some of the experiments, older mice were also examined. All experiments were conducted according to the institutional guidelines for animal welfare.

Two-dimensional microCT analysis of bone. Trabecular bone structure and bone volume (bone volume/tissue volume [BV/TV]) were examined based on two-dimensional micro X-ray computed tomography (microCT) analysis, using a microCT apparatus (Musashi; Nittetsu-ELEX). The fractional bone volume (BV/TV) was measured in a square area of 0.8 mm^2 (2,000 μm × 400 μm) in the distal metaphyseal region of the femora or the fourth lumbar vertebrate and was quantified using Luzex-F Image analyzing system (Nireco). The threshold for the measurements was set at 110 for the analyses as determined previously based on the correlation to the values to those obtained in histomorphological measurements (33).

ALP assay. Bone marrow cells were obtained by flushing out the cells from the medullary cavity of femora with α-minimum Eagle's medium (α-MEM). The cells were rinsed, counted, and plated in 96-well plates (5×10^4 cells/well) and were cultured in α-MEM supplemented with 10% FBS, 50 μg/ml ascorbic acid, 10 mM β-glycerophosphate, and antibiotics/antimycotics. In some of the cultures, the cells were treated with 100 ng/ml rh-BMP-2. Medium was changed every 3 d, and the cells were cultured for 10 d. The cells were rinsed twice with ice-cold PBS and scraped into 10 mM Tris-HCl containing 2 mM $MgCl_2$ and 0.05% Triton X-100, pH 8.2. The cell lysates were briefly sonicated on ice after two cycles of freezing and thawing. Aliquots of supernatants were subjected to ALP activity measurement and protein assay according to Bradford's method. In brief, aliquots of cell lysates were mixed with assay buffer containing 10 mM p-nitrophenyl phosphate in 0.1 M sodium carbonate buffer, pH 10, supplemented with 1 mM $MgCl_2$ and followed by an incubation at 37°C for 30 min. After adding 1 M NaOH, the amounts of p-nitrophenol liberated in the assay mixtures were measured using a spectrophotometer.

Mineralized nodule formation assay. Bone marrow cells were plated in 24-well plates (10^6 cells/well). The cells were cultured in α-MEM supplemented with 10% FBS, 50 μg/ml ascorbic acid, 10 mM β-glycerophosphate, and antibiotics/antimycotics (100 U/ml penicillin G, 100 μg/ml streptomycin sulfate, and 0.25 μg/ml amphotericin B; GIBCO BRL). Medium was changed every 3 d, and the cells were cultured for 2 wk. At the end of the cultures, the cells were fixed with 10% formalin/saline and stained for calcium with alizarin red S to identify mineralized bone nodules.

Osteoclastogenesis in bone marrow cultures. The proximal and distal epiphyseal ends were removed from femora, and bone marrow cells were flushed out. The number of total bone marrow cells was counted, and the cells were plated in 48-well plates (0.8 cm^2 per well) at a density of 5×10^5 cells/well. The cells were cultured in α-MEM supplemented with 10% FBS, 100 μg/ml antibiotics-antimycotics mixture, 10 nM $1,25(OH)_2$ vitamin D_3, and 100 nM dexamethasone. The medium was changed on day 3. TRAP-positive osteoclast-like multinucleated cells (greater than two nuclei) were counted at the end of 5 d of culture.

Histomorphometric analysis of bone. Osteoclast number per bone surface (Oc.N/BS, N/mm) and the percentage of osteoclast surface to bone surface (Oc.S/BS, %) were obtained by counting TRAP-positive cells and by measuring the area in serial 7-μm-thick sagittal histological sections of femora of wild-type ($n = 8$) and CIZ-deficient ($n = 6$) mice (8 wk old) at 200-fold magnification. TRAP-positive cells forming resorption lacunae on the surface of the trabeculae and containing one or more nuclei were identified as osteoclasts. For in vivo fluorescent labeling, calcein (1.6 mg/kg body weight) was intraperitoneally injected on days 0 and 4. Wild-type ($n = 8$) and CIZ-deficient ($n = 6$) mice (8 wk old) were killed on day 6. Femora were fixed in 99.5% ethanol and embedded in methylmethacrylate without decalcification. Sagittal histological sections (7 μm thick) were prepared, and the calcein images were visualized by fluorescent light microscopy. Histomorphometry of bone sections was performed using at least six optical fields within the secondary spongiosa. The abbreviations for histomorphometric parameters were according to the recommendation by the American Society of Bone and Mineral Research Histomorphometry Nomenclature Committee (34).

RNA extraction, cDNA synthesis, and PCR. Total RNA of whole humerus was extracted according to acid guanidium thiocyanate-phenol-chloroform method (35). First-strand cDNA was synthesized using 1 μg of

the total RNA and Molony murine leukemia virus reverse transcriptase. Primers were synthesized on the basis of the reported mouse cDNA sequences for GAPDH (GenBank/EMBL/DDBJ accession no. NM_008084), OPN (GenBank/EMBL/DDBJ accession no. AF515708), ALP (GenBank/EMBL/DDBJ accession no. AF285233), COL (GenBank/EMBL/DDBJ accession no. U38544), and OSX (GenBank/EMBL/DDBJ accession no. AF184902). Primers for PCR reactions were as follows: GAPDH, forward, 5′-ACCACAGTCCATGCCATCAC-3′ and reverse, 5′-TCCACCACCCTGTTGCTGTA-3′; OPN, forward, 5′-CGACGATGATGACGATGATGAT-3′ and reverse, 5′-CTGGCTTTGGAACTTGCTTGAC-3′; ALP, forward, 5′-ATTGCCCTGAAACTCCAAAACC-3′ and reverse, 5′-CCTCTGGTGGCATCTCGTTATC-3′; COL, forward, 5′-TTTGTGGACCTCCGGCTC-3′ and reverse, 5′-AAGCAGAGCACTCGCCCT-3′; and OSX, forward, 5′-CTGGGGAAAGGAGGCACAAAGAAG-3′ and reverse, 5′-GGGTTAAGGGGAGCAAAGTCAGAT-3′.

Amplification was performed at 21–25 cycles within a linear range. Each cycle was set at 94°C for 20 s; 60°C for 30 s; and 72°C for 40 s in a 25-μl reaction mixture containing 0.5 μl of each cDNA, 200 mM of each primer, 0.2 mM of dNTP, and 1 U Taq DNA polymerase (Takara). After amplification, 10 μl of each reaction mixture was subjected to electrophoresis to be analyzed on 1% agarose gel. The bands were visualized by ethidium bromide staining.

Measurement of bone mineral density. Bone mineral density (g/cm^2) of the entire femora was measured based on dual-energy X-ray absorptiometry (DEXA) using an apparatus specifically designed for small animals (PIXI; GE Lunar) equipped with a laptop computer. Calibration was performed using a standard block according to the manufacturer's instruction.

In vivo bone formation by direct BMP-2 injection. Direct injection of BMP-2 onto the calvariae was conducted as described previously (36). In brief, rhBMP-2 (5 μg in 20 μl saline) was injected onto the parietal bones of wild-type ($n = 8$) and CIZ-deficient ($n = 6$) mice (8 wk old). rhBMP-2 was obtained from the Genetics Institute. Injection was performed every other day for 10 d, and the animals were killed 1 d after the last injection. Calvariae were fixed in 4% paraformaldehyde in PBS, pH 7.4, for 24 h, removed from the skull, and subjected to soft X-ray examination. X-ray images were recorded and quantified by using a Luzex-F automated image analysis system (Nireco).

Statistical analysis. The results were presented as mean ± SEM, and statistical evaluation was performed based on Student's t test. p-values <0.05 were considered to be significantly different.

This research was supported by the Grants-in-Aid received from the Japanese Ministry of Education (21st Century Center of Excellence Program, Molecular Destruction and Reconstitution of Tooth and Bone, nos. 14207056, 16659405, 16027215, and 16022221), grants from Japan Space forum, NASDA, and Japan Society for Promotion of Science (Integrated Action Initiative in Core to Core Program, Research for the Future Program, Genome Science).

The authors have no conflicting financial interests.

Submitted: 3 June 2004
Accepted: 18 January 2005

REFERENCES

1. Gabriel, S.E., A.N. Tosteson, C.L. Leibson, C.S. Crowson, G.R. Pond, C.S. Hammond, and L.J. Melton III. 2002. Direct medical costs attributable to osteoporotic fractures. *Osteoporos. Int.* 13:323–330.
2. Stephen, A.B., and W.A. Wallace. 2001. The management of osteoporosis. *J. Bone Joint Surg. Br.* 83:316–323.
3. Kenny, A.M., and K.M. Prestwood. 2000. Osteoporosis. Pathogenesis, diagnosis, and treatment in older adults. *Rheum. Dis. Clin. North Am.* 26:569–591.
4. Doty, S.B., and E.F. DiCarlo. 1995. Pathophysiology of immobilization osteoporosis. *Curr. Opin. Orthop.* 6:45–49.
5. Takata, S., and N. Yasui. 2001. Disuse osteoporosis. *J. Med. Invest.* 48:147–156.
6. Gallagher, J.C. 2001. Role of estrogens in the management of postmenopausal bone loss. *Rheum. Dis. Clin. North Am.* 27:143–162.
7. Pavlin, D., S.B. Dove, R. Zadro, and J. Gluhak-Heinrich. 2000. Mechanical loading stimulates differentiation of periodontal osteoblasts in a mouse osteoinduction model: effect on type I collagen and alkaline phosphatase genes. *Calcif. Tissue Int.* 67:163–172.
8. Pavalko, F.M., N.X. Chen, C.H. Turner, D.B. Burr, S. Atkinson, Y.F. Hsieh, J. Qiu, and R.L. Duncan. 1998. Fluid shear-induced mechanical signaling in MC3T3-E1 osteoblasts requires cytoskeleton-integrin interactions. *Am. J. Physiol.* 275:C1591–C1601.
9. Nomura, S., and T. Takano-Yamamoto. 2000. Molecular events caused by mechanical stress in bone. *Matrix Biol.* 19:91–96.
10. Chiquet, M. 1999. Regulation of extracellular matrix gene expression by mechanical stress. *Matrix Biol.* 18:417–426.
11. Ziros, P.G., A.P. Gil, T. Georgakopoulos, I. Habeos, D. Kletsas, E.K. Basdra, and A.G. Papavassiliou. 2002. The bone-specific transcriptional regulator Cbfa1 is a target of mechanical signals in osteoblastic cells. *J. Biol. Chem.* 277:23934–23941.
12. Ikegame, M., O. Ishibashi, T. Yoshizawa, J. Shimomura, T. Komori, H. Ozawa, and H. Kawashima. 2001. Tensile stress induces bone morphogenetic protein 4 in preosteoblastic and fibroblastic cells, which later differentiate into osteoblasts leading to osteogenesis in the mouse calvariae in organ culture. *J. Bone Miner. Res.* 16:24–32.
13. Long, P., F. Liu, N.P. Piesco, R. Kapur, and S. Agarwal. 2002. Signaling by mechanical strain involves transcriptional regulation of proinflammatory genes in human periodontal ligament cells in vitro. *Bone.* 30:547–552.
14. Burger, E.H., and J. Klein-Nulen. 1999. Responses of bone cells to biomechanical forces in vitro. *Adv. Dent. Res.* 13:93–98.
15. Nakamoto, T., T. Yamagata, R. Sakai, S. Ogawa, H. Honda, H. Ueno, N. Hirano, Y. Yazaki, and H. Hirai. 2000. CIZ, a zinc finger protein that interacts with p130(cas) and activates the expression of matrix metalloproteinases. *Mol. Cell. Biol.* 20:1649–1658.
16. Thunyakitpisal, P., M. Alvarez, K. Tokunaga, J.E. Onyia, J. Hock, N. Ohashi, H. Feister, S.J. Rhodes, and J.P. Bidwell. 2001. Cloning and functional analysis of a family of nuclear matrix transcription factors (NP/NMP4) that regulate type I collagen expression in osteoblasts. *J. Bone Miner. Res.* 16:10–23.
17. Torrungruang, K., R. Shah, M. Alvarez, D.K. Bowen, R. Gerard, F.M. Pavalko, J.S. Elmendorf, K. Charoonpatrapong, J. Hock, S.J. Rhodes, and J.P. Bidwell. 2002. Osteoblast intracellular localization of Nmp4 proteins. *Bone.* 30:931–936.
18. Furuya, K., T. Nakamoto, Z.J. Shen, K. Tsuji, A. Nifuji, H. Hirai, and M. Noda. 2000. Overexpression of Cas-interacting zinc finger protein (CIZ) suppresses proliferation and enhances expression of type I collagen gene in osteoblast-like MC3T3E1 cells. *Exp. Cell Res.* 261:329–335.
19. Shen, Z.J., T. Nakamoto, K. Tsuji, A. Nifuji, K. Miyazono, T. Komori, H. Hirai, and M. Noda. 2002. Negative regulation of bone morphogenetic protein/Smad signaling by Cas-interacting zinc finger protein in osteoblasts. *J. Biol. Chem.* 277:29840–29846.
20. Shimizu, T., R. Mehdi, Y. Yoshimura, H. Yoshikawa, S. Nomura, K. Miyazono, and K. Takaoka. 1998. Sequential expression of bone morphogenetic protein, tumor necrosis factor, and their receptors in bone-forming reaction after mouse femoral marrow ablation. *Bone.* 23:127–133.
21. Usui, M., Y. Yoshida, K. Tsuji, K. Oikawa, K. Miyazono, I. Ishikawa, T. Yamamoto, A. Nifuji, and M. Noda. 2004. Tob deficiency superenhances osteoblastic activity after ovariectomy to black estrogen deficiency-induced osteoporosis. *Proc. Natl. Acad. Sci. USA.* 101:6653–6658.
22. McMahon, J.A., S. Takada, L.B. Zimmerman, C.M. Fan, R.M. Harland, and A.P. McMahon. 1998. Noggin-mediated antagonism of BMP signaling is required for growth and patterning of the neural tube and somite. *Genes Dev.* 12:1438–1452.
23. Hanada, T., and A. Yoshimura. 2002. Regulation of cytokine signaling and inflammation. *Cytokine Growth Factor Rev.* 13:413–421.

24. Ohlsson, C., K. Sjogren, J.O. Jansson, and O.G. Isaksson. 2000. The relative importance of endocrine versus autocrine/paracrine insulin-like growth factor-I in the regulation of body growth. *Pediatr. Nephrol.* 14:541–543.
25. Miyazono, K. 2000. Positive and negative regulation of TGF-beta signaling. *J. Cell Sci.* 113:1101–1109.
26. Moghal, N., and P.W. Sternberg. 1999. Multiple positive and negative regulators of signaling by the EGF-receptor. *Curr. Opin. Cell Biol.* 11:190–196.
27. Narita, T., K. Saitoh, T. Kameda, A. Kuroiwa, M. Mizutani, C. Koike, H. Iba, and S. Yasugi. 2000. BMPs are necessary for stomach gland formation in the chicken embryo: a study using virally induced BMP-2 and Noggin expression. *Development.* 127:981–988.
28. Sasai, Y., B. Lu, H. Steinbeisser, and E.M. De Robertis. 1995. Regulation of neural induction by the Chd and Bmp-4 antagonistic patterning signals in Xenopus. *Nature.* 376:333–336.
29. Merino, R., J. Rodriguez-Leon, D. Macias, Y. Ganan, A.N. Economides, and J.M. Hurle. 1999. The BMP antagonist Gremlin regulates outgrowth, chondrogenesis and programmed cell death in the developing limb. *Development.* 126:5515–5522.
30. Miyazono, K. 2000. Positive and negative regulation of TGF-beta signaling. *J. Cell Sci.* 113:1101–1109.
31. Yoshida, Y., S. Tanaka, H. Umemori, O. Minowa, M. Usui, N. Ikematsu, E. Hosoda, T. Imamura, J. Kuno, T. Yamashita, et al. 2000. Negative regulation of BMP/Smad signaling by Tob in osteoblasts. *Cell.* 103:1085–1097.
32. Nakamoto, T., A. Shiratsuchi, H. Oda, K. Inoue, T. Matsumura, M. Ichikawa, T. Saito, S. Seo, K. Maki, T. Asai, et al. 2004. Impaired spermatogenesis and male fertility defects in CIZ/Nmp4-disrupted mice. *Genes Cells.* 9:575–589.
33. Ishijima, M., S.R. Rittling, T. Yamashita, K. Tsuji, H. Kurosawa, A. Nifuji, D.T. Denhardt, and M. Noda. 2001. Enhancement of osteoclastic bone resorption and suppression of osteoblastic bone formation in response to reduced mechanical stress do not occur in the absence of osteopontin. *J. Exp. Med.* 193:399–404.
34. Parfitt, A.M., M.K. Drezner, F.H. Glorieux, J.A. Kanis, H. Malluche, P.J. Meunier, S.M. Ott, and R.R. Recker. 1987. Bone histomorphometry: standardization of nomenclature, symbols, and units. Report of the ASBMR Histomorphometry Nomenclature Committee. *J. Bone Miner. Res.* 2:595–610.
35. Chomczynski, P., and N. Sacchi. 1987. Single-step method of RNA isolation by acid guanidium thiocyanate-phenol-chloroform extraction. *Anal. Biochem.* 162:156–159.
36. Noda, M., and J.J. Camilliere. 1989. In vivo stimulation of bone formation by transforming growth factor-beta. *Endocrinology.* 124:2991–2994.